WORKSPACE VARIATION OF A HEXAPOD MACHINE TOOL

Joseph P. Conti[*], Charles M. Clinton[*], and Guangming Zhang
Department of Mechanical Engineering & Institute for Systems Research
University of Maryland,
College Park, MD 20742, USA

Albert J. Wavering
Intelligent Systems Division
National Institute of Standards and Technology
Gaithersburg, MD 20899, USA

ABSTRACT

A method is presented to evaluate the workspace variation of a Stewart platform based machine tool. Three sets of constraints, covering strut lengths, platform and base spherical joint angles, and strut collisions, are formulated using inverse kinematics. Recognizing the need to vary the platform orientation during machining, an algorithm to efficiently calculate the workspace is developed. Computer implementation provides a powerful tool to study the dynamic variation of the workspace as the spindle platform changes orientation. A case study is presented on the workspace variation of a prototype hexapod machine tool as a function of platform orientation. The results demonstrate the shift in size and location of the workspace as the platform orientation changes. The workspace analysis tools presented can be used to maximize the versatility of Stewart platform based machines and avoid violation of workspace constraint conditions.

1. INTRODUCTION

Improving product quality, reducing product cost, and shortening the product development cycle have always been critical for companies to stay competitive. These competitive drivers result in a continuing need to achieve improvements in accuracy, speed, and versatility in machining operations. These pressing needs pose challenges to the machine tool research community and have driven several machine tool companies to revisit some of their basic assumptions about machine tool design. As a result, prototypes of a new class of machine tools based on parallel kinematic structures have been introduced.

Among parallel mechanisms, the six degree-of-freedom Stewart platform has recently been used in a number of new machine tool designs (Stewart 1965). The Stewart platform is characterized by high force-torque capacity, high structural rigidity, and low moving mass. Several prototypes

[*] NIST Guest Researcher

of Stewart-platform-based machine tools, typically called hexapods, have been produced by Giddings & Lewis, Hexel Corporation, and the Ingersoll Milling Machine Company[1].

Although the versatility of hexapod machine tools has been recognized, their acceptance by industry as production equipment has not yet occurred. Some obstacles to this include their current high cost and unproven performance in a production environment. Furthermore, the fact that their workspace is not constant, but varies with platform orientation, means that in certain cases their use is not as straightforward as traditional machine tools.

During the past decade, several researchers (Gosselin 1990, Kumar 1992, Ji 1994, Luh et al. 1996) have performed studies of the workspace of Stewart platforms. Most of these studies focused on the workspace restrictions due to limited strut lengths and/or joint angles. Few of them have integrated other important constraints, such as avoiding strut collisions, into workspace modeling. In addition, little work has been done on determining dynamic variation of the workspace caused by changes in platform orientation. Such a study is essential since the variation of the platform orientation is an integral part of hexapod machining operations.

Recognizing the need to provide information for the planning of machining operations, this paper presents a new study to characterize the workspace of hexapod-type machine tools. In the analytical aspect, the paper presents the formulation of three constraint sets, including the consideration of strut collision, using the method of inverse kinematics. In the experimental aspect, numerical values of the limiting strut lengths and joint angles are taken from a prototype Octahedral Hexapod machine tool built by the Ingersoll Milling Machine Company and installed at the National Institute of Standards and Technology (NIST). Visualization of the workspace in 3-dimensional and 2-dimensional space is presented to depict the dynamic nature of the workspace as the platform changes orientation. To demonstrate the efficiency and robustness of the proposed approach, the workspaces obtained from the early work done by Gosselin (1990) and Luh et al. (1996) will be reconstructed.

2. STEWART PLATFORM WORKSPACE CHARACTERISTICS

When Stewart introduced his six degree-of-freedom mechanism in 1965, a reviewer of his paper suggested that the mechanism could provide the basis for a new type of machine tool. It has not been until recently, though, that computing power and control algorithms have reached the level of cost and sophistication necessary to make this idea feasible. However, efficient use of Stewart platform based machine tools requires operators and production engineers to have an understanding of how parallel mechanism machine tools carry out machining operations. In particular, a basic understanding of the machine's workspace will allow users to determine the suitability of hexapod machine tools to their own machining tasks. This knowledge will also allow users to identify locations of the machine tool's work volume where specific machining operations may take place.

For conventional machine tools, the concept of workspace is straightforward. It is usually a rectangular parallelepiped volume specified by three indexed numbers representing the maximum machine travel in the x, y, and z directions. The workspace remains unchanged during machining,

[1] Certain commercial equipment, instruments, and/or software are identified in this paper to describe the subject matter and to specify the experimental procedure adequately. Such identification is not intended to imply recommendation or endorsement by the National Institute of Standards and Technology, nor is it intended to imply that the equipment, instruments, or software identified are necessarily the best available for the purpose.

except when changes are made to the tool offset. For a Stewart platform, however, the irregularly shaped workspace varies in volume, shape, and position as the platform orientation changes. Such differences characterize the advantages and challenges presented to operators on the shop floor when using this new type of machine tool. For example, hexapod users may have to estimate the maximum size of parts able to be machined based on the complexity of the part geometry presented to them. Therefore, this workspace study is important in increasing the usability of hexapod machine tools.

Before we present the algorithm developed in this research to determine the workspace, we need to define the term *workspace* as the three-dimensional space the tip of the cutting tool can reach at a given platform orientation. For simplicity, in this research we define the workspace as the volume of space that the nose of the spindle can reach. The user can arbitrarily set the tool offset in the algorithm for specific workspace studies. Since an infinite number of platform orientations are possible, it follows that an infinite number of workspace plots may exist for a specific hexapod machine. This fact points out the necessity and importance of the work presented in this paper.

3. FORMULATION OF WORKSPACE CONSTRAINTS

The hexapod machine tool (Figure 1) located at the National Institute of Standards and Technology serves as a case study for our proposed method of workspace determination. As illustrated, the machine tool consists of a movable platform supported by six struts. A cutting tool, such as an end mill, is placed in the spindle of the movable platform. In this configuration,

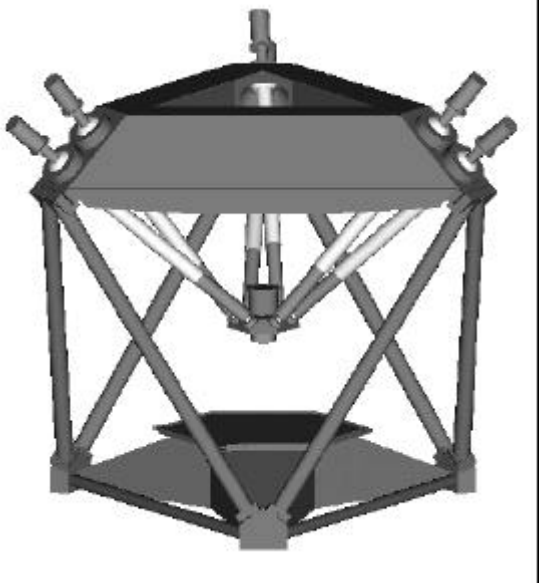

Figure 1. Solid model of Octahedral Hexapod machine installed at NIST (spindle motor not shown).

a part to be machined is fixed on the table and kept stationary during machining. It is the motion of the platform in three-dimensional space, which carries out the machining operation. Unlike most Stewart platforms, however, the hexapod under study inverts the 6-DOF movable platform and suspends it from an octahedral space frame. The workspace of this machine is defined by three constraints:

1. The limiting lengths, or maximum and minimum lengths of the six struts.
2. The limiting angular travel limits of the twelve spherical joints. Among them, six joints are associated with the stationary base; the other six joints are associated with the movable platform.
3. Possible collisions between individual struts.

To formulate the three constraint sets determining the workspace, the machine's inverse kinematics are calculated. For a given position and orientation of the platform in the three-dimensional work volume, the corresponding strut lengths and spherical joint angles can be determined (Fichter 1986). In this research, two coordinate systems, the base and the platform coordinate systems, are introduced, as illustrated in Figure 2. The position and orientation of the

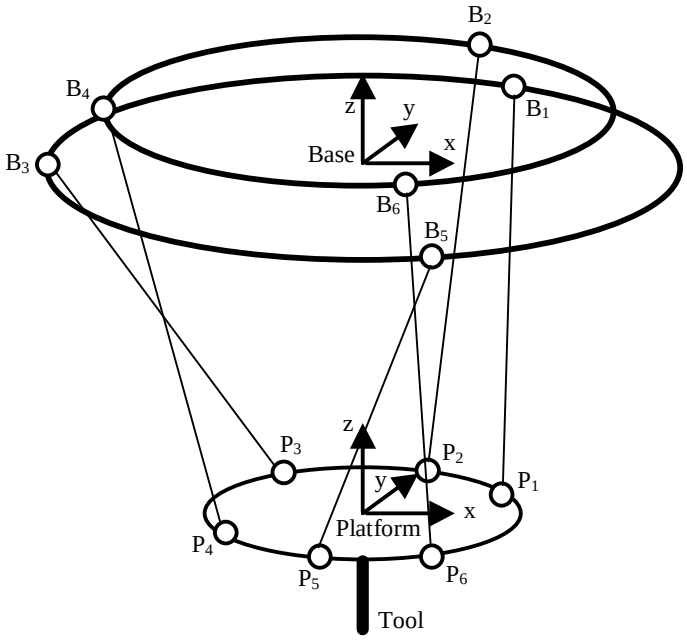

Figure 2. Base and platform coordinate systems.

movable platform can be represented by a position vector and a set of three angles in the base coordinate system as follows:

$$^{BASE}\bar{T} = \begin{bmatrix} T_x & T_y & T_z \end{bmatrix}^T \qquad \text{and} \qquad \mathbf{O} = (\alpha, \beta, \gamma),$$

where α =roll, β =pitch, γ = yaw. The Euler angle convention assumes that the platform is first rotated about the x-axis (roll), followed by rotation about the y-axis (pitch), and finally by rotation about the z-axis (yaw). The composite rotation matrix, $R_{\alpha\beta\gamma}$, is computed by pre-multiplication of the individual rotation matrices, R_α, R_β, and R_γ, namely,

$$R_{\alpha\beta\gamma} = R_\gamma R_\beta R_\alpha , \quad \text{where}$$

$$R_\alpha = \begin{bmatrix} 1 & 0 & 0 \\ 0 & \cos\alpha & -\sin\alpha \\ 0 & \sin\alpha & \cos\alpha \end{bmatrix} \quad R_\beta = \begin{bmatrix} \cos\beta & 0 & \sin\beta \\ 0 & 1 & 0 \\ -\sin\beta & 0 & \cos\beta \end{bmatrix} \quad R_\gamma = \begin{bmatrix} \cos\gamma & -\sin\gamma & 0 \\ \sin\gamma & \cos\gamma & 0 \\ 0 & 0 & 1 \end{bmatrix}.$$

In addition, the Stewart platform geometry gives us the positions of the six platform joints, $\mathbf{P_i}$, relative to the platform coordinate system, along with the six base joints, $\mathbf{B_i}$, relative to the base coordinate system, as illustrated in Figure 2. To calculate the platform joint position vectors in the base coordinate system, they must be rotated and translated. The rotation transform is given by:

$$^{R}\vec{P}_i = R_{\alpha\beta\gamma}\,\vec{P}_i \qquad \textit{for } i=1..6.$$

The translation transformation is a sum of the rotated platform vectors and the platform position vector, giving the position of the platform joints relative to the base coordinate system as follows:

$$^{BASE}\vec{P}_i = \vec{T} + {}^{R}\vec{P}_i .$$

As illustrated in Figure 3, the strut vectors, $\vec{S}_i$ are determined by:

$$\vec{S}_i = {}^{BASE}\vec{P}_i - \vec{B}_i .$$

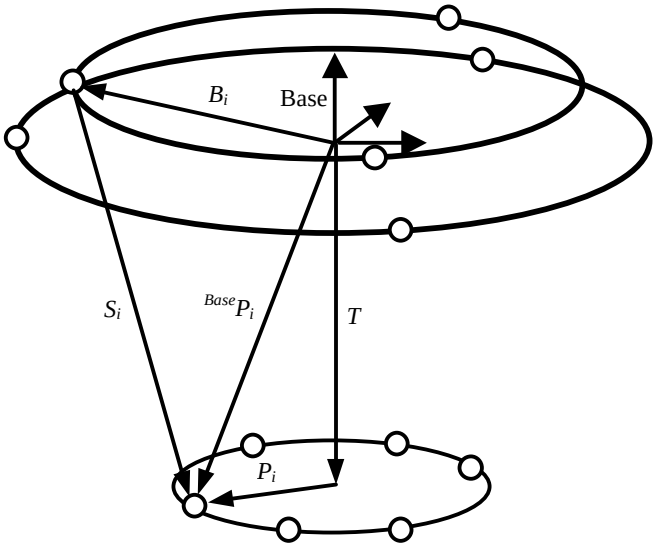

Figure 3. Inverse kinematic vectors.

3.1 Constraint Set I: Limiting Strut Lengths

Strut lengths, L_i, represent the first major workspace constraint for extensible-leg hexapod machines. They are computed using the following inverse kinematic equation:

$$L_i = \left|\vec{S}_i\right| = \left|\vec{T} + R_{\alpha\beta\gamma}\vec{P}_i - \vec{B}_i\right| .$$

For each of the six struts, its length must adhere to the following physical limits:

$$L_{\min} < L_i < L_{\max} \qquad \textit{for } i=1..6.$$

3.2 Constraint Set II: Spherical Joint Angular Limits

The hexapod under study has twelve spherical joints that connect the struts to the platform and base. As illustrated in Figure 2, six of these spherical joints are located on the platform, and the other six are on the base. These spherical joints allow the struts to freely change orientation as the platform moves. However, the spherical joints themselves are physically limited to a maximum angle (θ_{max}) due to the physical constraints of the spherical joints and to prevent collisions with the base structure.

Note that the spherical joint angles of the Stewart platform are measured relative to the *nominal strut vectors*. The strut vectors are nominal when the spherical joint angles (both base and platform) equal zero. The nominal strut vector simply provides a reference for spherical joint angle calculations. The six unit strut vectors, $\hat{s}_i$, and six nominal unit strut vectors, $\hat{s}_{i_{nom}}$, are determined by:

$$\hat{s}_i = \frac{\vec{S}_i}{\left|\vec{S}_i\right|}, \qquad \hat{s}_{i\,nom} = \frac{\vec{S}_{i\,nom}}{\left|\vec{S}_{i_{nom}}\right|} \qquad \textit{for } i = 1..6.$$

The magnitude of the base spherical joint angle is determined by:

$$q_{i\,Base} = \cos^{-1}\left(\hat{s}_i \cdot \hat{s}_{i_{nom}}\right) \qquad \textit{for } i = 1..6.$$

To determine the platform spherical joint angles, we first rotate the nominal unit strut vectors:

$${}^{R}\hat{s}_i = R_{a\,b\,g}\ \hat{s}_{i_{nom}}.$$

The dot product of the unit strut vector and the rotated nominal unit strut vector then gives the magnitude of the corresponding platform spherical joint angle as follows:

$$q_{i\,Platform} = \cos^{-1}\left(\hat{s}_i \cdot {}^{R}\hat{s}_{i_{nom}}\right) \quad \textit{for } i = 1..6.$$

It should be pointed out that the sphere angle of a spherical bearing has its allowable range because of its structural design. Therefore, the six base sphere angles and six platform sphere angles represent another important set of constraints to define the workspace of the hexapod machine tool. In other words, the base and platform sphere angles must adhere to the following physical limits. These constraints are given by

$$\left|q_{i\,Platform}\right| < q_{i\,Max\ Platform} \qquad \textit{for } i = 1..6,$$

$$\left|q_{i\,Base}\right| < q_{i\,Max\ Base} \qquad \textit{for } i = 1..6.$$

3.3 Constraint Set III: Avoiding Strut Collision

Examining Figure 1, the geometry of the hexapod under study does not preclude the possibility of collisions between the individual struts during the movement of the platform. Although somewhat simplistic, for the tools developed here it was deemed sufficient to evaluate this constraint by computing the mutually perpendicular distance between the (non-coplanar) strut centerlines and comparing it with a minimum value (slightly larger than the strut diameter).

To compute the mutually perpendicular distance between a pair of struts {i,j}, the following procedure is used (see Figure 4):

(1) A unit vector $\hat{u}$ normal to both strut vectors is computed:

$$\hat{u} = \frac{\vec{S}_i \times \vec{S}_j}{|\vec{S}_i \times \vec{S}_j|}.$$

(2) The distance between the two struts is determined using

$$D_{i,j} = \vec{r}_{ji} \cdot \hat{u},$$

where $\vec{r}_{ji} = \vec{B}_j - \vec{B}_i$.

It should be pointed out that with the geometry of the experimental hexapod shown in Figure 1, only strut collisions between the closely paired struts are a concern. This represents the final set of constraints on the work volume of the machine:

$$\{ D_{1,2} \;\; D_{3,4} \;\; D_{5,6} \} \geq D_{min}.$$

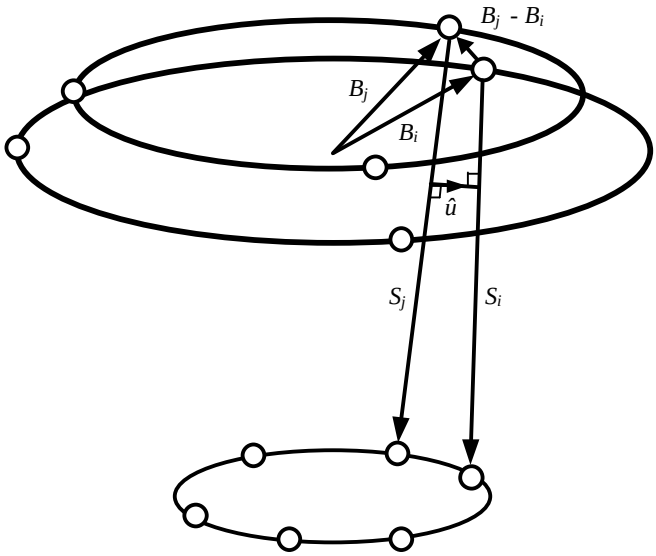

Figure 4. Vectors for computing the distance between strut centerlines.

3.4 Other Workspace Constraints

In this paper, we have presented the formulation of three constraint sets for determining the workspace of a particular hexapod machine tool, considering limitations on the strut lengths, joint angles, and strut collision. The algorithm presented should be able to include other forms of workspace constraints. Such constraints could be due to possible collisions of the struts with the part being machined or other external objects, and/or a different strut/joint arrangement than the hexapod machine tool used in the current investigation.

4. COMPUTER IMPLEMENTATION

The algorithm described in this paper was developed in the C++ language for its portability and object-oriented features. The Matlab software package was then used to graphically display the workspace. The entire implementation consists of five steps:

1. Define a function, called TestPose, which returns the evaluation result, either true or false.
2. Implement a search routine to determine the approximate workspace center.
3. Implement an error criterion to determine the workspace boundary.
4. Evaluate the workspace volume.
5. Graphically display the workspace.

4.1 TestPose Function

The *TestPose* function is defined as a Boolean function. The function tests an arbitrary position and orientation of the platform, or a pose of the platform, for constraint violation:

$$Boolean = \textbf{\textit{TestPose}}(\, T_x, T_y, T_z, \alpha, \beta, \gamma).$$

The function first computes inverse kinematics and then verifies whether the constraint sets I, II, and III are satisfied. If all of the constraints are satisfied, then the function returns a value of true. If any constraint is not satisfied, it returns a value of false. In other words, if the *TestPose* function is true, the given position and orientation of the platform is reachable by the hexapod.

4.2 Workspace Search Algorithm

The workspace algorithm conducts a search to determine the workspace of the hexapod machine tool with a given platform orientation, say $\mathbf{O}_1 = \{\alpha_1, \beta_1, \gamma_1\}$. The first step in the workspace search is to determine the approximate workspace center, a general requirement to initialize the workspace search. This is done by searching a three dimensional grid containing positions of the platform within the work volume of the machine. For the position at the center of the cube-shaped grid, the *TestPose* function checks for any constraint violations. Using the results obtained from testing these central positions, the approximate center of the workspace can be determined. This center will then serve as the origin of a spherical coordinate system used to define the actual workspace boundary (Figure 5). The major steps involved in the search process are outlined below.

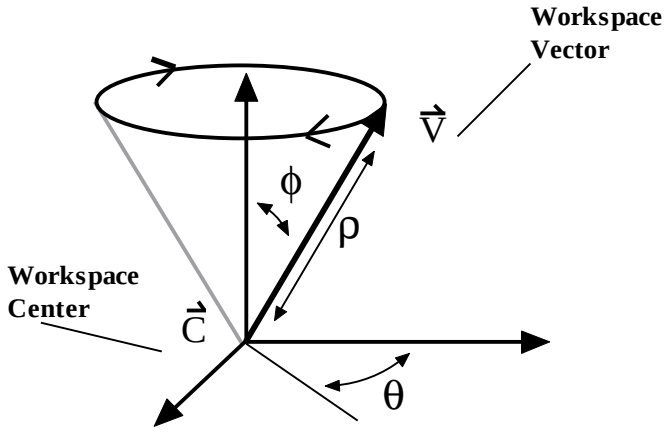

Figure 5. Workspace search vectors.

As illustrated in Figure 5, a workspace search vector, **V**, expressed in the spherical coordinates, $\mathbf{V} = \{\rho, \theta, \phi\}$, is introduced. The vector, **V**, is considered to be at or near the workspace boundary if the following workspace boundary condition is satisfied:

Workspace Boundary Condition

TestPose$(r, \theta, \phi, \mathbf{O}_1)$ *= True,*

TestPose$(r + \varepsilon, \theta, \phi, \mathbf{O}_1)$ *= False.*

The process of searching the entire space is accomplished by rotating the search vector in discrete intervals $\Delta\theta$ and $\Delta\phi$. The algorithm is presented by the following pseudocode.

Spherical Search Algorithm

```
θ = 0°
loop while θ < 360°
        φ = -90.0°
        loop while φ < 90°
                find the radius that satisfies the Workspace Boundary Condition
                φ = φ + Δφ
        end loop
        θ = θ + Δθ
end loop
```

4.3 Workspace Boundary Algorithm and Error Analysis

The workspace search algorithm is based upon finding a ρ that represents the boundary of the workspace. The algorithm to determine this boundary depends on one assumption made in this research regarding the geometry of the workspace map. We have assumed that if a point (θ,ϕ,ρ_1) is found to violate the hexapod machine tool constraints, all points (θ,ϕ,ρ_2) such that $\rho_2>\rho_1$ will also violate the hexapod constraints. Based on this assumption, the procedure for finding the boundary can be given by the following pseudocode for a successive approximation approach:

Workspace Boundary Algorithm

```
r = value outside of the workspace
Δr = r/2
loop while Δr > ε/2
        if TestPose(θ,φ,r, O1) = true
                r = r + Δr
        otherwise
                r = r - Δr
        Δr = Δr/2
end loop
if TestPose(θ,φ,r, O1) = false
        r = r - ε.
```

In terms of the accuracy at the end of the search process, Figure 6 graphically depicts the variation of the search vector at the final stage of the search process. As illustrated, the search

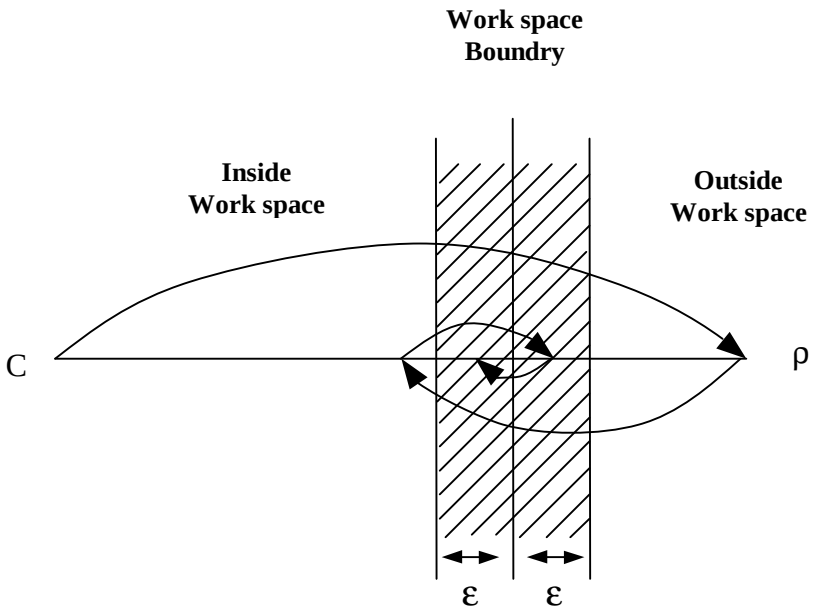

Figure 6. Search algorithm error.

vector changes in ρ until $\Delta r \leq \varepsilon/2$ is reached, where ε is set to 1.0 mm in the current work. This guarantees that ρ is within $\pm\varepsilon$ of the workspace boundary (Figure 6). The last step in the procedure is to subtract the final value of ρ by ε (if necessary) to guarantee that **V** lies within the workspace boundary. Thus, the possible error of the search algorithm at each point is between zero and -ε.

4.4 Evaluation of the Workspace Volume

The workspace map is defined by numerous data points, **V**, centered about a search origin, **C**. Let a *sector* be defined by four adjacent workspace data points**, {$\mathbf{V_1}$, $\mathbf{V_2}$, $\mathbf{V_3}$, $\mathbf{V_4}$}** and the workspace search origin, **C**, as illustrated in Figure 8. Summing the volume of all unique *sectors* determines the total volume of a workspace map. The volume of a sector (Figure 7) is approximated as a four-sided pyramid by the following method:

1. Determine the average length of these four vectors:
$$r_{av} = \frac{r_1 + r_2 + r_3 + r_4}{4}.$$
2. Approximate the arc lengths as the base and width of the pyramid:
$$base = \Delta f \cdot r_{av},$$
$$width = \Delta q \cdot r_{av}.$$
3. The height of the pyramid is given by
$$height = \sqrt{\left(r_{av}^2 - \frac{\left(width^2 + base^2 \right)}{4} \right)}.$$

4. The volume of a specific sector can be approximated using the known base, width, and height and is given by

$$V_{\text{sector}} \approx V_{pyramid} = \frac{base \times height \times width}{3} .$$

5. The total workspace volume is determined by summing the calculated volumes of all the sectors.

$$V_{workspace} = \sum_i V_{\text{sec}tor_i}$$

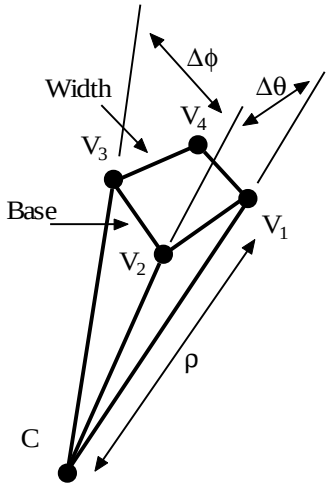

Figure 7. Workspace volume calculation.

The error of this method for computing the volume of a sphere was examined by comparing it to the analytical solution (for a sphere of radius 1),

$$V_{\text{sphere}} = {}^4/_3 \, \pi \, r^3 = 4.1888 \quad where \; r = 1 .$$

Table 1 displays sphere volume calculations when various numbers of sectors are used. As expected, the error of the volume calculation algorithm decreases as the number of sectors that define a workspace map increases. The error using 1200 sectors is approximately 0.5%. The error is likely to be greater than this when the algorithm is used to compute actual workspace map volume, since the algorithm probably works best for a sphere, and the actual hexapod workspace maps deviate significantly from a spherical shape. Also, the results given in Table 1 below do not include the contribution of errors in the radius estimates.

Table 1. Sphere Volume Error Analysis.

Sectors	Volume	% Error	Runtime
40	3.6962	11.8	t_o
180	4.0676	2.9	2 t_o
760	4.1586	0.7	18 t_o

1200	4.1695	0.5	38 t_o

5. DISCUSSION OF RESULTS

5.1 Hexapod Workspace Plots

Figure 8a presents the workspace of the hexapod machine tool for a horizontal platform orientation. As shown in this figure, the upper half of the workspace is predominantly defined by the minimum strut length limit. The middle section of the workspace is defined by the base spherical joint angle limits and the bottom of the workspace is defined by maximum strut lengths. For a horizontal platform orientation, the workspace boundary is not determined by the platform joint angle limits or strut collisions. These constraints, however, become prominent for platform orientations with large rotation angles.

Figure 8b gives a workspace simulation for a platform roll about the x-axis of 10º. The general shape is similar to the previous workspace with the exception of the platform joint limits. This platform orientation shifts the overall workspace in the positive *y* direction. This shifting trend continues with 20º of roll (Figure 8c). In this case, the negative *y* side of the workspace becomes defined primarily by platform sphere limits. The hexapod workspace continues to shift in the positive *y* direction as the platform roll deviates from the horizontal orientation.

An important aspect of the hexapod machine tool is that some sets of platform orientations lead to workspaces, which share no regions of overlap. Figure 9 displays three workspace plots for three different platform orientations. This workspace characteristic means that the machine cannot necessarily move from one position and orientation to another in an arbitrary fashion. This example highlights the need to carefully plan and check tool paths with orientation changes.

In addition to the hexapod under study, the method of workspace determination presented in this paper can be applied to various other Stewart platforms. The workspace of the INRIA prototype (Gosselin 1990) for a horizontal platform orientation is presented in Figure 10. This figure was created using the workspace program with the geometry and workspace constraints of the INRIA Stewart platform. This workspace plot compares well with the analytical plot produced by Gosselin.

The workspace of a Spatial Stewart Platform described in Luh et al. (Luh 1996) is graphed in Figure 11. This machine is used for flight simulator applications and is not limited by joint angle constraints.

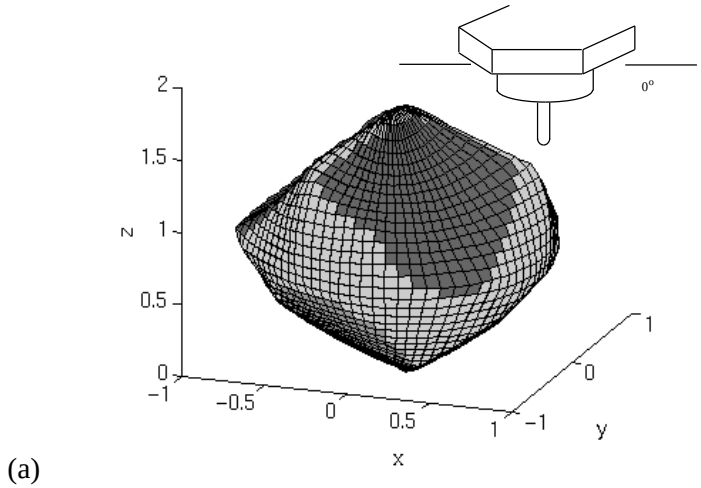

(a)

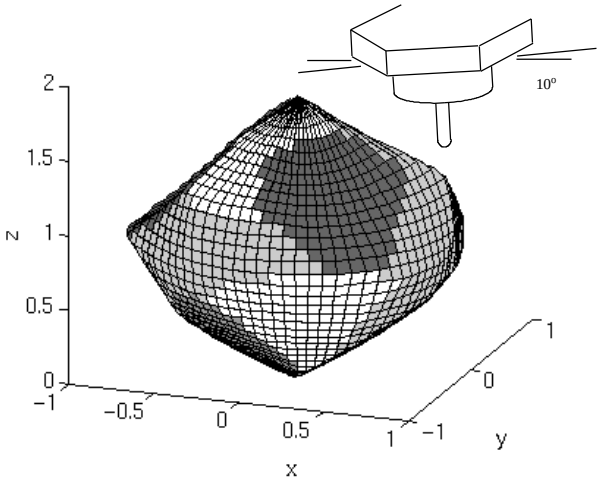

(b)

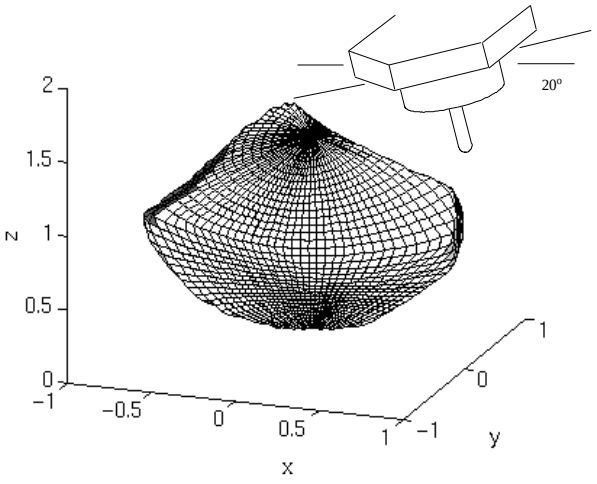

(c)

Figure 8. Hexapod workspace examples (all dimensions in meters).

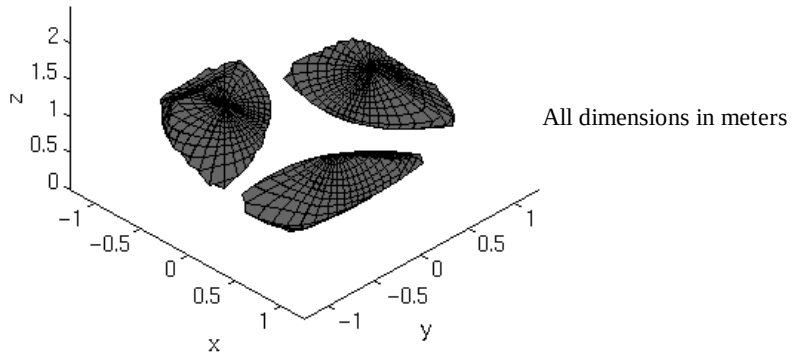

Figure 9. Workspaces for (roll = 28°, pitch = 0°), (roll = -13.6°, pitch = 24.7°), and (roll = -13.6°, pitch = 24.7°).

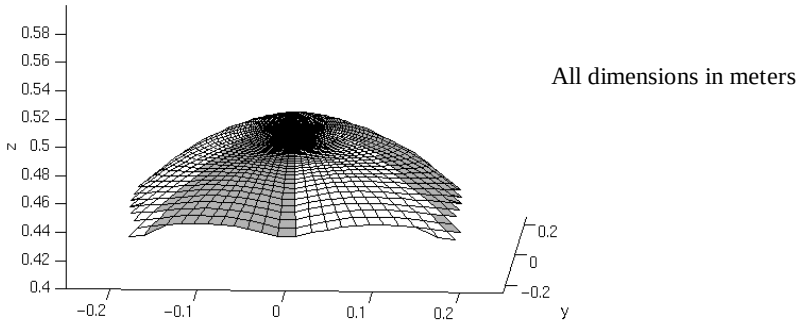

Figure 10. Workspace for INRIA Stewart platform—horizontal platform orientation (Gosselin 1990).

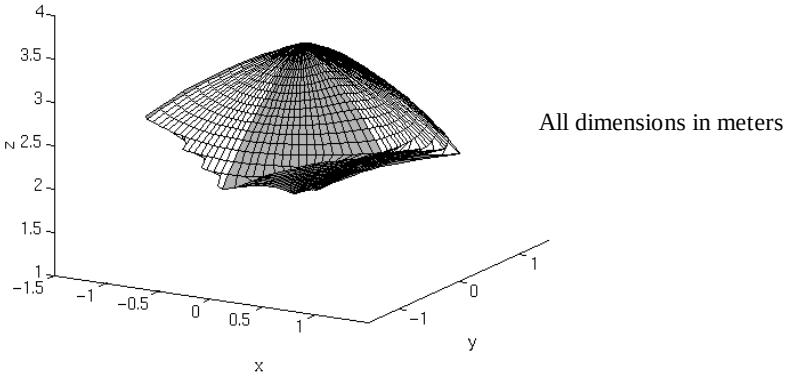

Figure 11. Workspace for spatial Stewart platform—horizontal platform orientation (Luh 1996).

5.2 2-D Area Plots of Workspace

Quantitative insight into the workspace of the hexapod machine tool at NIST can be obtained by plotting the cross section of the workspace at various heights. Figure 12 displays cross sections of the hexapod workspace as the platform rolls from 0º to 20º. These plots represent the cross section at three different heights, -2.6, -2.1, and -1.6 meters, measured from the base (upper) coordinate system of the machine. Examining the two-dimensional plots, we see that the cross sectional area decreases and shifts its location in the positive *y* direction as the platform rolls (rotates about the x-axis).

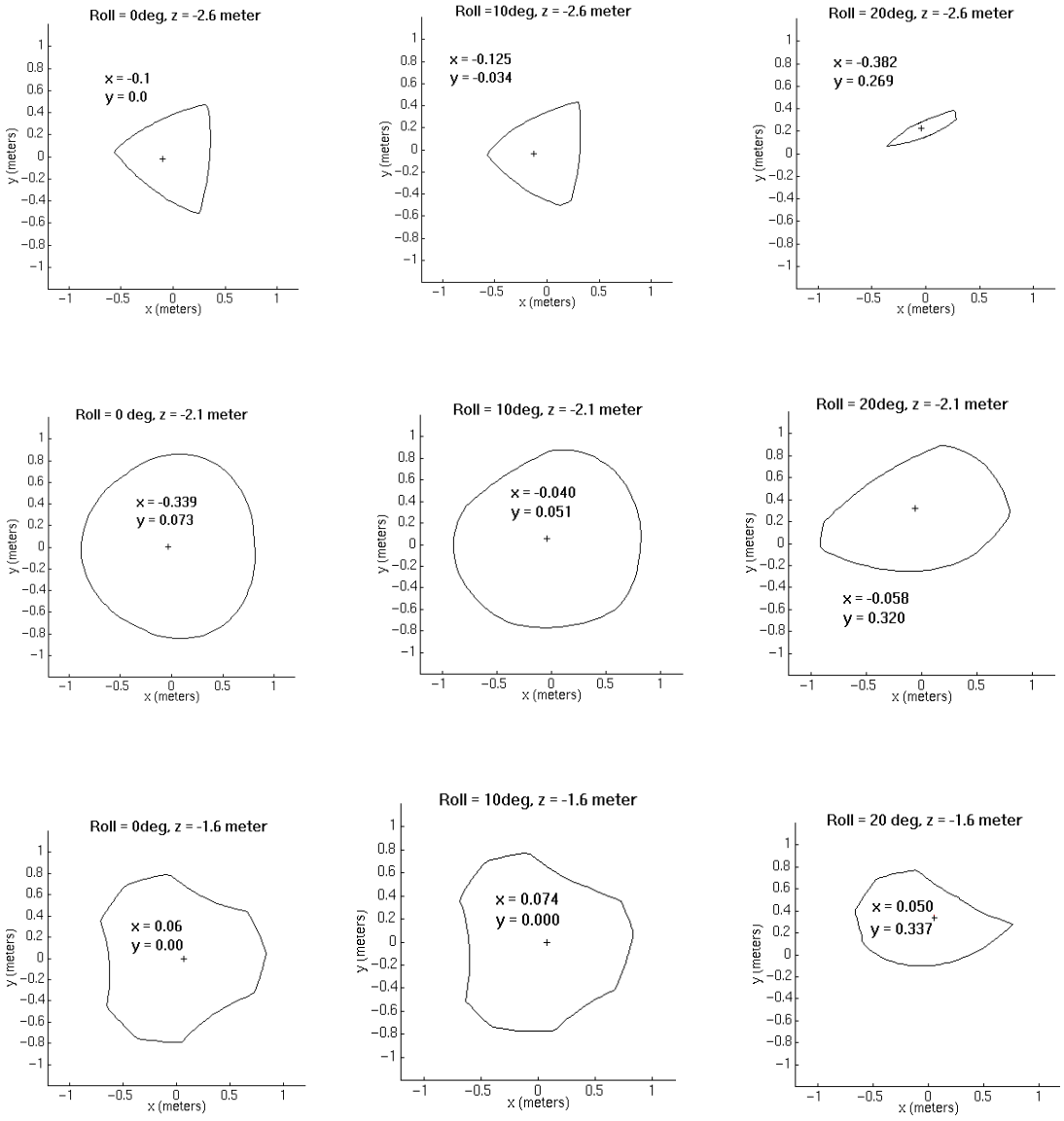

Figure 12. Workspace slices for hexapod at NIST (Z = -2.6, -2.1, and -1.6 meters in base coordinates).

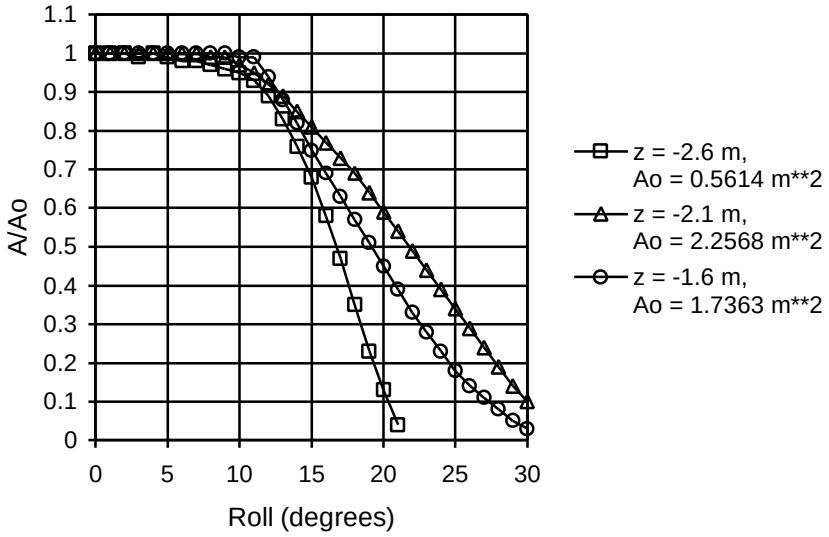

Figure 13. Variation of X-Y workspace area as a function of spindle platform roll.

Figure 13 displays the normalized cross sectional areas of the hexapod's workspace as a function of roll for z levels of -2.6, -2.1, and -1.6 meters (again, in base coordinates). Inspection of the plots clearly shows that a rapid reduction in cross sectional area occurs at a roll of approximately 11º. Before this point, however, the cross sectional area remains more or less constant. This points out the fact that the available workspace may be significantly reduced when the production of complex contoured parts calls for large orientation changes of the spindle platform.

The calculations of workspace volume further demonstrate the workspace variation due to spindle platform orientation changes. Figure 14 plots the workspace volume of the hexapod machine tool as a function of roll. For a vertical spindle, the workspace has a volume of approximately 2.4 cubic meters. The volume remains essentially constant until a roll angle of 11º is reached. Beyond 11º, the workspace volume decreases in an approximately linear fashion. The rapid decrease in workspace volume for platform roll beyond 11º is primarily due to the platform

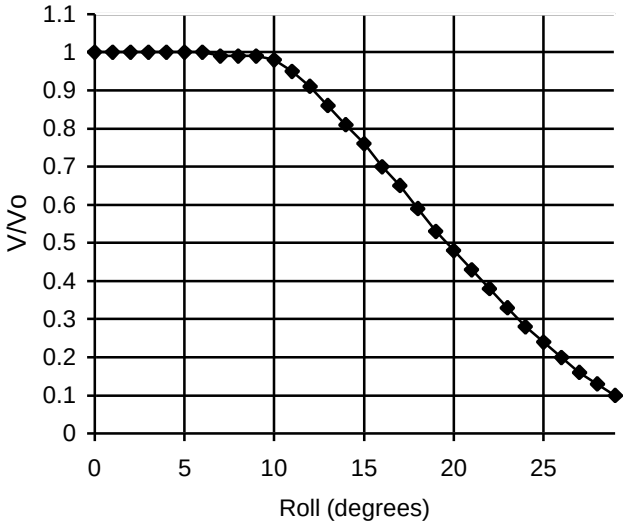

spherical joint angle constraint.

Figure 14. Workspace volume as a function of spindle platform roll (V_0 = 2.3965 m^3).

6. CONCLUSIONS

A method to determine the workspace of a Stewart platform using a numerical spherical search has been presented and a case study completed using the experimental prototype Octahedral Hexapod machine at NIST. Workspace plots show that as the platform orientation of the hexapod increases, the overall workspace volume decreases. Thus, a tool path that requires large platform rotations will be more constrained in available workspace than tool paths with near vertical platform orientations.

The numerical search method was applied to two other Stewart platforms previously explored by researchers. Reconstructed workspace plots match the solutions developed by other researchers. More importantly, this method of workspace determination is beneficial in designing new Stewart platform based machines. The workspace for alternative platform configurations may be explored by simply entering the machine geometry. With a runtime of less than one minute, the workspace plots can be quickly generated and examined.

7. FUTURE WORK

One difficulty in presenting workspace research is that an infinite number of workspace plots exist for most Stewart platform based machines. However, one cannot expect to examine all possible workspace figures to gain an understanding of the machine. The difficulty lies in communicating the characteristics of the workspace of a machine with the fewest number of workspace plots. This is essential in order to compare the performance of different parallel linked mechanisms. For example, if hexapod machine A has a larger workspace for a horizontal platform than hexapod machine B, it does not necessarily mean it has a greater workspace at other platform orientations. A standard method to represent the workspace of Stewart platform and other machines with coupled translational and rotational degrees of freedom needs to be developed.

8. REFERENCES

Fichter, E.F., 1986, "A Stewart Platform Based Manipulator: General Theory and Practical Construction", *International Journal of Robot Research*, 5(2): 157-182.

Gosselin, C., 1996, "Determination of the Workspace of 6-DOF Parallel Manipulators," *Journal of Applied Mechanical Design*, Vol. 112, 331-336.

Hunt, K. H., 1983, "Structural Kinematics of In-Parallel-Actuated Robot Arms", *Trans. ASME J. of Mechanisms, Transmissions, and Automation in Design*, 105:705-712.

Ji, Z., 1994, "Workspace Analysis of Stewart Platforms via Vertex Space," *Journal of Robotic Systems*, 11(7), 631-639.

Kumar, V., 1992, "Characterization of Workspaces of Parallel Manipulators," *ASME Journal of Mechanical Design*, Vol. 114, 368-375.

Lebert, G., Liu, K., Lewis, F.L., 1995, "Dynamic Analysis and Control of a Stewart Platform Manipulator", *Journal of Robotic Systems*, 10(5), 629-655.

Luh, C., Adkins, F., Haung, E., and Qiu, C., 1996, "Working Capability Analysis of Stewart Platforms", *ASME Journal of Mechanical Design*, Vol. 118, 220-227.

Stewart, D., 1965, "A Platform with six degrees of freedom", *Proc. Inst. Mech. Engineering*, 371-386.

Wang, J., 1992, *Workspace Evaluation and Kinematic Calibration of Stewart Platforms*, Ph.D. Dissertation, Florida Atlantic University, Department of Mechanical Engineering.